Forestry: An International Journal of Forest Research, 2025, 1–16
https://doi.org/10.1093/forestry/cpaf034
Original Article

Costs and precisions of alternative plot configurations for estimating above-ground tree biomass in tropical forests

Erkki O. Tomppo[1,*], Bryan C. Foster[2], Laura S. Kenefic[3], Mark J. Ducey[4]

[1]Department of Forest Sciences, University of Helsinki, Latokartanonkaari 7, P.O. Box 27, Helsinki FI-00014, Finland
[2]Foster Forestry and Environmental Consulting LLC, 123 Chipman St., South Burlington, VT 05403, United States
[3]United States Department of Agriculture, Forest Service, Northern Research Station, 54 Government Road, Bradley, Maine 04411, United States
[4]Department of Natural Resources and Environment, University of New Hampshire, 114 James Hall, 56 College Road, Durham, NH 03824, United States

[*]Corresponding author. Department of Forest Sciences, University of Helsinki, Latokartanonkaari 7, P.O. Box 27, Helsinki FI-00014, Finland.
E-mail: erkki.tomppo@helsinki.fi

Abstract

We used field measurements and sampling simulations with existing tree-level data to assess the precision of the estimates and data measurement costs for ground-based sampling inventory for above-ground tree biomass (AGB) and basal area estimation. Data were obtained from primary wet tropical forests using field measurements in Costa Rica and, for simulations, published tree-level data on Barro Colorado Island in Panama. Plot configurations and costs were compared using criteria commonly used by forest carbon offset project developers to meet precision of +/−10% at 90% confidence interval for AGB estimation. Detached plots were tested using circular fixed-area, nested, and several types of angle-count configurations. A plot divided into a cluster of sub-plots was further tested with angle-count plots. The basal area factor (BAF) used for angle-count plots varied between 2 and 20. Key findings include (i) angle-count plots emerged as a highly efficient plot configuration for forest inventories in tropical regions with high tree density and size variability with 33%–80% cost savings without precision penalties compared to the nested and fixed-area plots respectively; (ii) angle-count plots with large BAFs (3–8) are cost-efficient and can achieve low sampling errors (~10%) with fewer plots and trees than the fixed-area and nested plots; (iii) a cluster of angle-count subplots with a large BAF (e.g. BAF = 12, 16, 20) is an efficient configuration for further investigation; (iv) small fixed-area plots for small trees with angle-count sampling for large trees is also an efficient configuration for further investigation. Among the alternative plot configurations compared, angle-count plots with their variants emerged as a highly cost-efficient and versatile alternative in complex tropical forests with visual occlusion, and are worth studying further.

Keywords: forest inventory; carbon monitoring; fixed-area plots; angle-count plots; precision; neotropical forests

Introduction

Global change and the possible role of forests in mitigating climate change is a pressing research topic. The International Union for Conservation of Nature's Nature-based Climate Solutions financially incentivize source avoidance and sink enhancement of greenhouse gas emissions via forest activities that generate offset credits (Pasgaard et al. 2016). The three major intervention types for Forest Carbon Offset (FCO) projects include: conservation such as Avoided or Reduced Emissions from Deforestation and Degradation (REDD), enhancement such as Afforestation and Reforestation, and sustainable management such as Improved Forest Management (Griscom et al. 2017, Forest Carbon Offsets 2023). FCOs require frequent monitoring, reporting, and verification including on-the-ground inventories prior to verification audits every 5–6 years over 40–100-year lifespans (Foster et al. 2017, Pan et al. 2022). All major global FCO standards (American Carbon Registry, Climate Action Reserve, Gold Standard, Plan Vivo, and Verified Carbon Standard) require verifiers to check ground-based inventory plots scaled up to the project level—a "stratify and multiply" approach using expansion factors (Marvin and Asner 2016). The Intergovernmental Panel on Climate Change has articulated a simple "stock change difference" method to calculate emission factors (Achard et al. 2014) between two measurements of spatially permanent plots over time.

Two key questions in any forest inventory are what type of sample plot layout (sampling design) and plot configuration (plot type and size) are most appropriate to be used (Schreuder et al. 1993, Gregoire and Valentine 2007, Kershaw Jr. et al. 2016). Many forest inventories use fixed-area plots, but fixed-area plots are known to be cost-inefficient for assessing forest volume and carbon stocks when the volume or carbon of the individual trees

Handling editor: Dr. Fabian Fassnacht
Received 20 January 2025; **revised** 16 May 2025; **accepted** 19 May 2025

Table 1. Plot configurations and sampling designs widely used by tropical forest carbon offset project developers. Dbh = diameter at breast height.

Plot configurations	Fixed	Fixed	Nested	Nested
Plot sizes	0.1 ha, (0.02 ha regeneration optional)	Varies 0.25–1.0 ha	0.5 ha, 0.2 ha, 0.1 ha, (0.005 ha regeneration optional)	0.13 ha, 0.062 ha, (0.03 ha regeneration optional)
Clustering	No	No	Yes, 4 sub-plots, centers 50 m N-E-S-W	Optional
dbh thresholds	10 cm, (2 cm regeneration optional)	2.5–10 cm	50 cm, 20 cm, 10 cm, (0.1 cm regeneration optional)	50 cm, 20 cm, (5 cm regeneration optional)
Plot shape	Rectangular	Circular or Rectangular	Rectangular	Circular
Manual date	2014	2021	2015	2018
Manual source	**Costa Rica NFI** https://www.sirefor.go.cr/pdfs/VOLUMEN-2.-MANUAL-DE-CAMPO-INVENTARIO-FORESTAL-NACIONAL.pdf	**Forestplots.net** https://forestplots.net/upload/publication-store/itm_172/ForestPlotsnet_et_al_Taking_the_pulse_of_Earths_tropical_forests_BiologicalConservation_June2021.pdf	**Panama NFI (0.5 ∗ FAO)** https://chm.cbd.int/api/v2013/documents/05B386D2-5BCD-A52D-6097-F853803CC619/attachments/205145/Inventario%20Nacional%20Forestal%20-%20Resultados%20Fase%20Piloto%202013-2015.pdf	**Winrock** https://winrock.org/wp-content/uploads/2013/08/Winrock_Terrestrial_Carbon_Field_SOP_Manual_Feb2018.pdf

varies widely because a large number of trees would be measured that do not significantly contribute to the volume or carbon stock (Schreuder et al. 1993, Gregoire and Valentine 2007, Kershaw Jr. et al. 2016). However, measuring small trees may be important for other purposes, such as biodiversity assessments and predicting the future development of forests. Tropical FCO developers typically use the plot configurations and sampling designs shown in Table 1 for estimating above-ground biomass (AGB).

In tropical forests high AGB and dense wood are strongly correlated with the presence of large trees (Nam et al. 2018). Although leaf-level metabolic productivity declines with tree age, expanding total leaf area maintains carbon storage (Stephenson et al. 2014), while consistent overall stocking, comprised of trees with broad age and height distributions, maintains a large carbon sink at stand and landscape levels (Hardiman et al. 2013). Ali et al. (2019) call this phenomenon the "big-sized tree effect." Allocating measurement time for these big trees could improve the efficiency of ground-based inventories. ForestGEO plots in primary forests from boreal to temperate and tropical biomes (ForestGeo 2025) suggest that the biggest 1% of trees in terms of diameter ("big trees", ≥30–60 cm depending on the biome) contribute 25%–50% of AGB. The share of AGB as a function of breast height diameter approximately follows an exponential function (Lutz et al. 2018, Piponiot et al. 2022). In central South America, south-east Asia and central Africa, trees ≥70 cm diameter constitute only 1.5%, 2.4%, and 3.8% of total trees per hectare (TPH) respectively but contribute 25%, 39%, and 45% of estimated AGB (Slik et al. 2013). Bastin et al. (2018) and Sullivan et al. (2017 and 2018) reported that the 20 largest trees per hectare predicted AGB and tree density with a relative error of 17.7% and 4%, respectively. In wet tropical forests of Costa Rica, where we conducted our field work, trees ≥60 cm diameter constituted only 2.5% of the TPH but contributed 25% of estimated AGB (Clark et al. 2019).

One way to allocate the measurement efforts to the trees that have largest contribution to the variables of interest, such as AGB, is to employ unequal sampling strategies. Walker et al. (2018) recommend a commonly used plot type, nested plots, with unequal inclusion probabilities in Winrock's "Standard Operating Procedures for Terrestrial Carbon Measurement": a small plot for trees with small diameter at breast height (dbh) concentric within one or more larger plots for trees with larger dbh. Nested plots enhance efficiency relative to non-nested fixed-area plot designs, because the inclusion probabilities for individual trees are correlated with tree basal area (g) as a target variable.

Selection of the sample plot configuration, including shape and size, in naturally regenerated tropical forests is a challenging task due to the high ecological variation both at local and regional scales (Roveda et al. 2016, Pinto et al. 2021). Various factors, e.g. gap-dynamic and corresponding light conditions, host-specific fungal diseases, and adaptations to microclimatic, edaphic, and topographic variables, all drive high spatial heterogeneity in tropical forests (Kricher 2017). Visual occlusion caused by dense understory creates additional difficulties.

Fixed-area plots have often been studied and used in tropical forests. Pinto et al. (2021) studied the optimal sample plot size for estimating basal area and carbon stock versus biodiversity using four test sites in tropical forests in Brazil. They noticed that different tropical forest vegetation types present different optimal sample plot size but those are similar for basal area and carbon stock, while estimates of biodiversity variables were not sensitive to plot size. Examples of earlier studies focusing on optimal field plot designs in tropical forests include Oliveira et al. (2011) and da Silva et al. (2003), which also aimed to obtain accurate and cost-effective estimates by identifying optimal plot sizes.

An old and widely used method to make sampling-based forest inventories efficient is to employ inclusion probabilities proportional to size (PPS) in sampling. In PPS sampling, a tree's probability of being included is proportional to some dimension of a tree, e.g. basal area (g), that is, the cross-sectional surface area of a tree at breast height. When basal area is used as the dimension, i.e. the most common method of PPS sampling, the method is called angle-count sampling, horizontal point sampling or Bitterlich sampling after its inventor Walter Bitterlich (Bitterlich 1948, Mesavage and Grosenbaugh 1956, Grosenbaugh and Stover 1957). The method has been widely used in national forest inventories (NFIs) and forest management inventories particularly in boreal and temperate forests, and also for AGB, basal area, and merchantable volume estimation (Packard and Radke 2007, Ducey 2009, Tomppo et al. 2010, Smelko 2013, Alijanpour et al. 2018). Several types of instruments have been developed to determine the inclusion of an individual tree. Although angle-count plots have been documented in the tropics (Banyard 1975, Schreuder et al. 1987, Sullivan et al. 2014, Palace et al. 2015, 2016) their use in tropical forests is rare. In part, this may be due to concerns over visual occlusion of tree stems by dense understory vegetation and very large trees.

The use of angle-count sampling and plots is rarer in the tropics than in temperate forests. One reason could be that forest inventories need to provide estimates for several forest variables, not only volumes and biomass, but also tree diameter distributions and trees densities, for example. These variables can be estimated using angle-count plots without bias, although the error estimates for small trees tend to be large. Angle-count methods also need special attention and care in change estimation. Examples of using angle-count plots in the tropics include Druszcz et al. (2010) and Lionjanga and Pereira (2014), see also Torres and Lovett (2013).

One more fact that may affect the selection of the plot configuration and sampling methods, particularly the use of angle-count methods, is a possible non-circularity of tree stem cross-sections. Pulkkinen (2012) developed methods for quantifying the systematic and sampling errors associated with common ways of selecting diameter within non-circular cross-sections, e.g. overestimation in volume estimates. Pulkkinen also proposed methods to overcome the problem. Non-circularity could be more common in the tropics than in the temperate and boreal zones, although full circularity in theory is also rare in the other regions.

Another method to increase the efficiency of an inventory, particularly in multi-purpose inventory, is to use adaptive sampling and adaptive cluster sampling, e.g. to sample clustered and rare events (Roesch 1993). Netto et al. (2017) suggested the method in forest inventories of the volume of commercial tree species in the Brazilian Amazon. A similar advantage can be achieved when a plot is divided into a cluster of sub-plots, particularly when the events (i.e. objects of interest, such as large or valuable trees), are sparsely distributed but not clustered. An example of estimators for an angle-count plot consisting of a cluster of subplots, or when sub-plots overlap, is presented by Van Deusen and Grender (1989).

Note that cluster sampling in which plots are arranged in clusters, as often employed in NFIs, is an example of a sampling design beyond our research questions. The purpose of cluster sampling is also to decrease the inventory costs without increasing sampling errors. The penalty is the spatial dependence of the variables of the observations on the nearby plots and thus the decrease of new information of the observations. One of the key questions is thus the distance between the plots in a cluster or the distance between the sub-plots in a plot configuration. These questions of detached plots versus a cluster of plots or cluster of sub-plots, including the design parameters, are also relevant to large-area inventories, such as NFIs in which near-optimal solutions have been sought. Examples of the design parameters in the NFIs are plot size, number of plots in a cluster, cluster shape, and distance between plots in a cluster (Tomppo et al. 2010, 2014, Yim et al. 2015, Kershaw Jr. et al. 2016, Picard et al. 2018, Lister and Leites 2022).

The focus of this study is finding efficient plot configurations, particularly for AGB estimation. We chose wet tropical forests for our research, as these forests are among the world's largest AGB stocks, sinks, and sources (Harris et al. 2021). Field measurement costs in these forests are high for trees with diameters ≥50 cm above buttresses, i.e. when ladders are needed for diameter measurement (Cushman et al. 2021a), and for trees with heights ≥35 m in closed canopies (Hunter et al. 2013), i.e. when crowns are difficult to distinguish with a hypsometer. The potential savings with efficient plot configurations are thus high. Tropical forests provide inventory challenges that are different from those encountered in temperate and boreal forests, where plot configurations have been studied more widely.

Although studies using angle-count plots in the tropics exist, for example Mora-Espinoza et al. (2020) showing superiority of angle-count sampling in teak plantations, our paper is the first to our knowledge to examine clusters of angle-count sub-plots as opposed to clustered fixed-area plots. An improved cost efficiency of a cluster of subplots can also be expected due to weak spatial correlation in naturally regenerated tropical forests (Fig. 2). Even nearby subplots bring new information. Angle-count sampling with maximum inclusion distance, that is, truncated angle-count plots, mitigates the problems caused by visual occlusion.

The specific objective of this study was to compare the precision of the estimates and field measurement costs (hereafter, efficiency) of alternative plot configurations, i.e. plot sizes and shapes, in estimating AGB and basal area of trees in tropical forests. The three basic plot configurations tested were fixed-area circular plot, nested circular plot, and angle-count plot. In particular, the performance of large basal area factors (BAFs) in angle-count sampling in tropical forests was studied. We also compared total costs of selected plot configurations when aiming for a given estimation precision with a given confidence interval and regular grid of plots. Field measurements were used together with a separate full census tree dataset for sampling simulations. Detached plots, consisting of one plot, and a plot divided into sub-plots were tested with fixed-area plots, nested plots, and several types of angle-count plots.

Materials and methods

Datasets

Two types of datasets were utilized in our studies: our own field measurements and existing full census data. The latter were used for sampling simulation. Field work was necessary to calculate travel, measurement and establishment time costs, and to test angle-count sampling in the tropics despite visual occlusion. The field site allowed us to project the results to the larger sampling simulation site. Both sites represent wet primary tropical forest on the Caribbean side of southern Central America.

Field site

For field work in 2024, we chose an accessible neotropical research facility, La Selva Biological Station of the Organization for Tropical

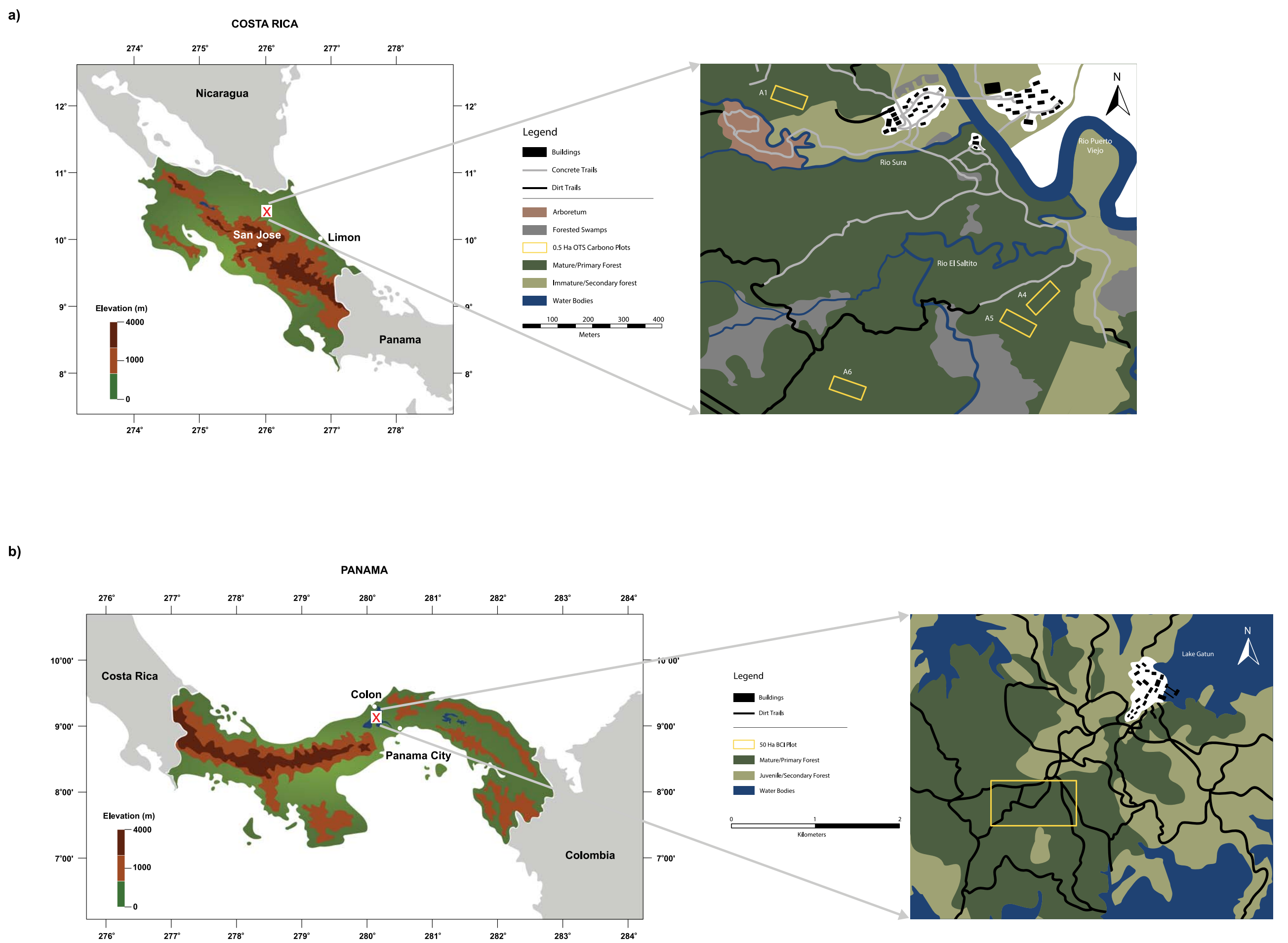

Figure 1. Locations of primary neotropical forest sites including (a) 0.4 ha subsampled from 2 ha at OTS-Costa Rica in 2024 which we used for field data collection, and (b) 50 ha full tree census at BCI-Panama in 2015 which we used for sampling simulations.

Studies (OTS), with 1550 ha of conserved tropical forest. La Selva is in the Heredia province in the Atlantic lowlands of Costa Rica near the town of Puerto Viejo de Sarapiquí (McDade et al. 1994) (10°26’N, 83°59’W). The annual minimum and maximum daily average temperatures at La Selva range from 19°C to 31°C, on average, and mean annual rainfall of 4500 mm with a dry season from March–April (Clark and Clark 2011). We used the Carbono research unit that has a 20-year sampling history focused on forest carbon flows and stocks (hereafter the OTS-Costa Rica site) (Clark and Clark 2021). Four of the six rectangular (100 m × 50 m) Carbono plots (2 ha in total) were selected within a 71.3-ha alluvium stratum at ∼100 m above sea level (Fig. 1a) (Clark and Clark 2000). Two of the six plots, A2 and A3, were excluded due to numerous blowdowns during Hurricane Nate in 2017; these blowdowns dramatically reduced AGB (Cushman et al. 2021b). Mature trees in the alluvium stratum exceed 500 years of age, based on radiocarbon dating (Fichtler et al. 2003). In total 50 tree species were identified on the plots, though *Pentaclethra macroloba* dominated with 47% contribution to basal area (Table S1). The next 12 genera contributed 2%–5% each to basal area.

Sampling simulation site

Sampling simulation studies were carried out using full census tree-level data from 2015. We chose a relatively nearby site on Barro Colorado Island near the town of Gamboa, Panama (McDade et al. 1994) (9°15’N, 79°85’W) (Fig. 1b), managed by the Smithsonian Tropical Research Institute (hereafter the BCI-Panama site). The annual minimum and maximum daily average temperatures range from 23°C to 32°C, on average, and the mean annual rainfall 2600 mm with a dry season from January–April (Leigh 1999). The 50-ha (1000 × 500 m) forest dynamics plot has flat topography on a highly weathered Ultisol soil at ∼130 m above sea level (Condit 1998). The coordinates of each tree were recorded in the census, making sampling simulation possible for different plot configurations. Only tree-level variables, dbh, above-ground biomass (AGB, tons) and basal area (BA, m^2), in addition to tree coordinates were utilized. There were 328 tree species on the site, of which the 15 most abundant genera contributed 60% to the basal area with *Quararibea asterolepis* (Malvaceae), *Prioria copaifera* (Fabaceae) and *Alseis blackiana* (Rubiaceae) being the most abundant species (Table S2). Basic forest statistics are shown in Table 2.

Data collection and data preparation

We conducted field work at OTS-Costa Rica to measure plot establishment and measurement times and to check comparability of results from different plot configurations. We used an Apple© Ipad Pro 28 cm on a chest pack to minimize data transcription errors and to compare current data against previous data from plot configurations. Dual SkyPro© GPS pocket receivers with the Avenza Maps© application were used for navigation along with the Theodolite© application for true (declination-adjusted) orientation.

Table 2. Basic statistics as a function of tree-level diameter at breast height (dbh) thresholds at the 50-ha Barro Colorado Island, Panama site. TPH = number of trees per ha, G = basal area, AGB = above-ground biomass.

dbh threshold cm	TPH	G-weighted mean dbh, cm	G $m^2 ha^{-1}$	AGB Mg ha^{-1}
0	8470.26	NA	31.59	305.64
1	4154.24	58.5	31.59	305.64
5	1007.96	61.5	29.90	301.15
10	416.58	66.1	27.40	290.59
20	150.26	74.9	22.89	263.16
30	79.34	83.4	19.54	235.05
40	45.52	92.7	16.37	203.98
50	27.38	102.8	13.54	172.78
100	3.14	157.4	5.04	64.39

Time measurements were made with an iPad/iPhone Stopwatches© application and included travel (to plots from the border of the site, between plots and also back to the border of the site), establishment of the plots, and measurements on the plots (cf. Zeide 1980). Travel speed was calculated to be 2.0 km h^{-1}. The order of implementation of the methods was rotated in plots so that bias from advance knowledge of the trees was eliminated. A team consisted of three people, as an additional person was required for diameter measurements on ladders above buttresses in the tropical site. A rate of 25.00 USD $person^{-1}$ h^{-1} for experienced field assistants was paid in 2024 (this rate includes 25% labor tax, resulting in a tax-free rate of 18.75 USD). Note that efficiency comparisons between any two sets of plot configurations are insensitive to specific cost used, because the same hourly costs apply to all configurations; other conclusions of the paper about cost can easily be re-scaled for other hourly cost values. Four additional field costs independent of sampling design were excluded from analysis: administration and logistic planning time; field equipment; transport and travel time to the sampling site; and room and board near the sampling site. We consider these fixed costs that would be incurred irrespective of plot configuration as opposed to configuration dependent variable costs.

A Haglof© Vertex Laser Geo 360° with T-4 ultrasound transponder was used to measure distances to establish fixed-area circular plot perimeters. Flagging at plot radius at cardinal directions proved inadequate in mature tropical forest; therefore, plot establishment involved setting a white string around the perimeters of fixed-area and nested plots with the Vertex monopod as plot center. The Vertex instrument was calibrated on the first field day at the 10 m mark with a fiberglass tape. Establishment of angle-count plots consisting of sub-plots involved planting red-painted 0.5-m long, 0.6-cm diameter polyvinyl chloride pipe at four points in cardinal directions.

The tree-level variables measured regardless of configuration were: tree numbers from tags or paint to confirm genus and species, dbh (to nearest 0.1 cm) and total tree height (to nearest 1 m). A synthetic fabric diameter tape was used for tree diameter measurements; the tape was tested for accuracy on the first field day with its reverse distance against a fiberglass tape. For tree diameter above buttresses in the tropics, we used 1 or 2 segments of a 2-m aluminum ladder to measure diameters above buttresses, at 3 or 6 m above the ground level depending on the length of buttresses. In cases where allometric equations employ height (in addition to diameters and species-related specific gravity), AGB accuracy can be improved by 7%–13% with height measures (Chave et al. 2003, 2014, Feldpausch et al. 2012, Larjavaara and Muller-Landau 2013). The Vertex was used for tree height measurements; the accuracy of height measurement was tested by measuring two mature trees 15–30 m tall in an open area and subsequently measuring the same trees with an altimeter from a DJI Mini 4 © drone. In the plots, the transponder was positioned at 1.3 m vertical distance from the ground on the uphill side of the tree and the Vertex hypsometer was carried a horizontal travel distance of approximately one half to one tree length.

On circular fixed-area plots and nested plots, we flagged all trees that belonged to the sample based on the diameter threshold after the diameters were measured and recorded together with species on the first 360° round. On the second 360° round, heights were measured and recorded and flagging removed.

BAFs used on angle-count plots were selected using the known forest characteristics of the study sites. The BAFs were 3 and 12; the latter one was used to measure height for a sub-sample of the trees on which dbh was measured. To determine inclusion on angle-count plots, prisms were sighted at the diameter measurement height (1.3 m, 3 m, or 6 m). We marked all "in" and "borderline" trees with flagging on the first 360° round. For "borderline" trees, we measured the distance from a plot center to the closest tree face using the Vertex transponder. One conventional angle-count shortcut is counting every other "borderline" tree, but this often produces significant error (Iles and Fall 1988, Holdaway et al. 2014). We removed flagging from all "borderline but out" trees. For "in" diameter trees we only removed flagging after recording diameter and then added a strip of different colored flagging for Big BAF for subsample height measurement "in" trees. On the second 360° round, we measured and recorded height for the newly flagged trees then removed the flagging after height recording.

Estimation methods

The main purpose of the study was to compare different plot configurations, particularly in AGB and basal area estimation. We compared the precisions and costs to assess the efficiencies of the alternative plot configurations. We focused comparisons on the estimates of mean values per unit area, that is, the values of the quantities per hectare. The areas of the study sites were known, so we omitted area estimation and used the known areas in estimates for inclusion probabilities and per unit area estimates. Further, plot-level estimates were derived from tree-level data using standard methods (e.g. Kershaw Jr. et al. 2016). We also calculated the estimates and error estimates for AGB and BA for some plot configurations using OTS-Costa Rica field data to compare the performance of the plot configurations from

Table 3. Plot configurations and sampling designs used at the Organization of Tropical Studies La Selva, Costa Rica site. BAF = basal area factor, TC = total count, VBAR = volume to basal area ratio, dbh = diameter at breast height, POM = point of measure of 3 m or 6 m above-ground to reach above buttresses.

	Fixed-area plot reference	Nested plot	Angle count cluster plot points
Size of each plot	0.1 ha	0.1 ha 0.025 ha	Cluster of 4 sub-plots N-S, E-W 25.2 m apart; 3 BAF TC trees; 12 BAF for VBAR trees
Total number of plots	4	4	4
dbh thresholds and maximum distance	≥10 cm dbh or POM 17.8 m radius	≥30 cm dbh or POM 17.8 m radius plot ≥10 cm dbh or POM 8.9 m radius plot	≥10 cm dbh or POM 17.8 m truncated distance
Rule used to select trees for height measurements	All dbh measured trees	All dbh measured trees	All "in trees" with a BAF of 12

the two sites. Additionally, quadratic mean diameter (QMD) was calculated using those data (e.g. Kershaw Jr. et al. 2016).

In the OTS-Costa Rica site, tree-level ABG (Mg), including palms, and denoted by agb, was calculated using the equation

$$agb = \left(0.0673 \bullet \left(w_d \bullet h \bullet d^2\right)^{0.976} /1000\right)/2 \qquad (1)$$

where w_d is dry wood species specific gravity in g cm^{-3}, d is tree diameter (cm) and h is total tree height (m) (Chave et al. 2014, p. 6). For w_d, we used values from Data dryad: Toward a worldwide wood economics spectrum (Zanne et al. 2009). For the BCI-Panama simulation data, estimates of agb and g were already provided in the data, with agb based on Eq. 1. (Piponiot et al. 2024, Condit et al. 2019).

Plot configurations used in field measurements and sampling simulations

Field measurements were used mainly to assess measurement costs and precision, to compare efficiencies of the alternative plot configurations in sampling simulations. Plot configurations widely used by FCO projects (Foster et al. 2017) were utilized in selecting the plot configurations both for the field measurements and sampling simulations, in addition to plot configurations based on our own efficiency tests. Diameter at breast height (or diameter above buttress) of living trees and height by species were measured in the field.

When using sampling simulation, the three basic plot configurations were, as given above, fixed-area circular plot, nested circular plot, and angle-count plot (Tables 3 and 6–8 in the Results section). With angle-count plots, several variants were tested. The details are listed in the next section. All simulations and analyses were carried out using the R programming language (version 4.2.0, R Core Team 2021).

Estimating sampling errors and number of plots needed when using sampling simulations

Several plot configurations, that is, plot sizes and shapes, with different dbh thresholds were analyzed (Tables 6–8). (Here, we employ the term "dbh thresholds" for simplicity, while noting that for some trees diameter is measured above buttresses.) The basic plot types were (i) a circular fixed-area plot with sizes of 0.025, 0.05, 0.1, and 0.25 ha, (ii) a nested circular plot with two sizes and two dbh thresholds, the larger circle 0.1 ha and the smaller one either 0.05 or 0.025 ha, (iii) an angle-count plot with BAF 3 to 12, (iv) a cluster of nested plots, (v) a cluster of two or four angle-count subplots. With angle-count plots, we also tested truncated variants in which a fixed maximum distance for inclusion replaced the usual angle-count distance. This effectively converts the truncated angle-count to a fixed-area plot for trees of sufficient size, limiting the errors caused by occlusion and improving efficiency (Eqs. 3 and 4). The dbh thresholds and other details are given in Tables 6–9.

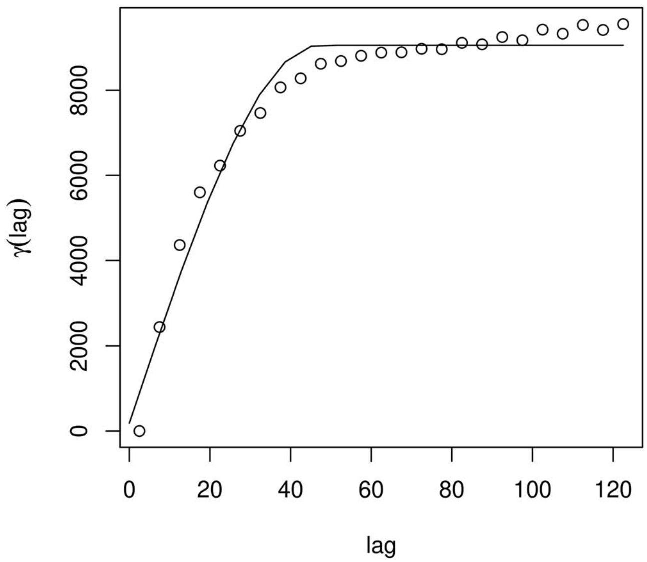

Figure 2. Estimated semivariance based on the BCI-Panama data on an angle-count plot with a BAF of 3, with a fitted model, range = 46.9 m, sill = 9055 and nugget effect = 185.2.

After the first simulation tests, the sampling designs selected for detailed analyses were 32 field sample plots or clusters of sub-plots on a regular grid of 8 × 4 plots and with plot distances of 120 m in both south–north and west–east directions (Tables 6 and 7). These distances are long enough to make sure that the plot-level AGB estimates are independent with the plot configurations used (Fig. 2). Other plot configurations were also considered, such as those used by FAO and other organizations in the tropics (Table 1), however a 100 m × 500 m half FAO plot could hardly fit in the 1000 m × 500 m simulation site.

The simulations were done as follows: A total of 40 different samples were selected from the tree-level data. The start corner of the first sample grid was as near as possible to the southwest corner of the test site. The corner was first shifted by 3 m steps to the east (eight times) and after that 2 m steps to north (four times) starting from the westernmost position of the test site. Such small shifts were needed to fit all plots in all 40 samples inside the test site. The samples thus covered the entire test site. The inclusion of a tree in a sample was determined based on the coordinates and dbh of that tree.

The sampling errors were estimated as the standard deviations of the estimates calculated over the samples following the definition of sampling error (Eq. 6). We focused on mean values per hectare of forest characteristics. For mean values, totals were first calculated using the Horvitz-Thompson estimator (Horvitz and Thompson 1952) estimator that employs inclusion probabilities (Eq. 5). The inclusion probability of a tree k for circular plots, including angle-count plots, can be written

$$p_k = \rho\pi\, r_k^2 \tag{2}$$

where r_k is the radius of the plot from which the tree is included in the sample and ρ the intensity of the plot centers, that is, the number of plots, n, divided by the area of the inventory site, here 50 ha. Thus $\rho = n/(50*10\,000)$ when r_k is given in meters. The value of r_k is constant for the fixed-radius plot and depends on the tree diameter for the nested plot.

$$r_k = \frac{50d_k}{100\sqrt{q}} \tag{3}$$

and for a truncated angle-count plot

$$r_k = \min\{\,50d_k/100\sqrt{q}, r_{max}\} \tag{4}$$

where d_k is the breast height diameter of tree k, r_{max} the maximum distance from which any tree is included into the sample and q the BAF.

The unbiased Horvitz-Thompson (1952) estimator of the total value of variable y_i based on the sample i is thus

$$\hat{y}_i = \sum_{k\in S_i} \frac{y_{i,k}}{p_{i,k}} \tag{5}$$

where S_i is the set of the trees in the sample i. The mean value on forest land is obtained by dividing the estimate in Eq. 5 by the known forest area A.The estimate of the sampling error of the mean values can be assessed by the standard deviation of the estimates over the samples, that is, by the standard deviation of the $\hat{\bar{y}}_i$ values:

$$\text{sampling error} = \sqrt{\frac{1}{n_S}\sum_{i=1}^{n_S}\left(\hat{\bar{y}}_i - \hat{\bar{y}}\right)^2} \tag{6}$$

where $\hat{\bar{y}} = \sum_i^{n_S}\hat{\bar{y}}_i/n_S$ and n_S is the number of the samples.

When using field data, the sampling error was estimated as the standard error of the plot-level estimates and assuming them to be independent. We note that under the design-based inference framework of most forest inventories, independence arises from the independence of plot selection; spatial autocorrelation is irrelevant (Gregoire 1998).

One simple way to assess and compare the efficiency, E, of a plot configuration is to define E as:

$$E = c \bullet V(Y)^2 \bullet TC \tag{7}$$

where V(Y) is the estimate of the sampling error of variable Y, TC the total costs and c a selected scaling quantity, here 10^{-7}. Since the same scaling quantity c is applied to all plot configurations, relative comparisons (i.e. whether one configuration is more efficient than another) do not depend on c. The use of c is purely for convenience, so that E is rescaled not to have very large values.

Total costs were calculated using the cost components from OTS-Costa Rica site field data and applied to BCI-Panama site simulation data. The costs for measurements in a continuous forest inventory of permanent plots, e.g. 5-year monitoring and verification during 50-year FCO project longevity and discounted to the present, were calculated using the equation

$$TC_{50,d} = \sum_{i=0,5}^{50} TC_i \bullet \left(1+\frac{p}{100}\right)^{-i}, \tag{8}$$

where $TC_{50,d}$ is the total cost discounted to the present time point, TC_i the cost at time point i, p the interest rate (%), and summation goes from 0 to 50 in 5-year intervals.

For estimating the number of plots needed for a given confidence interval in a simple way when estimating the average AGB and stand-level basal area per hectare (G), we assumed that the plot-level variables of AGB, and respectively G, are independently and identically distributed with a mean μ and a variance σ. The independence assumption was justified for the data. The correlation coefficients of the variables AGB and G in the consecutive plots, with a distance of 75 or 120 m, were – 0.025 and – 0.035, respectively. Inspection of robust semivariances confirmed the spatial independence of plot-level AGB and G observations at the distances of greater than 20 m when using the estimator by Cressie and Hawkins (1980).

$$\hat{\gamma}(r) = \frac{\left(1/N(r)\sum_{S(r)}|z(x)-z(y)|^{1/2}\right)^4}{0.914+0.988/N(r)}, \tag{9}$$

where r is the distance of the observations (lag), $N(r)$, the number of observations with the distance of r, and $z(x)$ and $z(y)$ are the values of the variable of interest (e.g. AGB) at the points x and y respectively. An example of an estimated semivariance is shown in Fig. 2. The value of range here is 46.9 m meaning that the semivariance levels off at that distance and first reaches 95% of the sill, the asymptotic value of the semivariance.

Let us recall some basic statistical concepts and introduce notations to estimate the number of plots needed for a given target precision. Let us denote the sample standard deviation by s. The length d of a two-sided confidence interval corresponding to a confidence level of 100 $(1-\alpha)$% calculated from the sample is thus

$$d = 2 \bullet z_{\alpha/2} \bullet \frac{s}{\sqrt{n}} \tag{10}$$

where $z_{\alpha/2}$ is a percentage point from N(0,1)-distribution, and the number of the observations needed

$$n = \frac{4 \bullet z_{\alpha/2}^2 \bullet s^2}{d^2} \tag{11}$$

Note that the Eqs. 10 and 11 hold for large sample sizes of 30 or larger. Percentage points from t-distribution should be used for small sample sizes.

Table 4. Between-plot travel speed in the study site, within-plot establishment time, and measurement time and cost in US dollars (USD) for experienced field assistants at Organization of Tropical Studies La Selva, Costa Rica, 2024. FP = fixed-area plot, NP = nested plot, AC = angle-count. The time and cost from the place of accommodation and offices to the field site was excluded.

Work phase	Average time, hour (minutes)	Costs per field crew (USD)
Travel per km	0.5 (30)	\$12.50/km/person × 3 people = \$37.50/km
FP establishment for 0.1 ha	0.7 (42)	\$25/person/hour × 3 people = \$75 × 0.7 h = \$52.50/FP
NP establishment for 0.1 ha, 0.025 ha	1.1 (66)	\$25/person/hour × 3 people = \$75 × 1.1 h = \$82.50/NP
AC cluster plot establishment for 4 sub-plots	0.3 (18)	\$25/person/hour × 3 people = \$75 × 0.3 h/4 sub-plots = \$5.60/AC sub-plot
FP tree measurement		\$25/person/hour × 3 people = \$75 × 0.02–0.05 = \$1.5–3.75
diameter only,	0.02 (1.2),	
height and diameter	0.05 (3)	
NP tree measurement		\$25/person/hour × 3 people = \$75 × 0.02–0.05 = \$1.5–3.75
diameter only,	0.02 (1.2),	
height and diameter	0.05 (3)	
AC cluster plot of 4 sub-plots		\$25/person/hour × 3 people = \$75 × 0.02–0.07 = \$1.5–5.25
tree measurement	0.02 (1.4),	
diameter only, height and diameter	0.07 (4.2)	

Table 5. Efficiency of alterative fixed-area plot (FP), nested plot (NP) and angle-count cluster plot (AC cluster plot of 4 sub-plots) configurations calculated using field sampling data from Organization of Tropical Studies La Selva, Costa Rica, 2024. All alternatives use the same numbers of plots or clusters of sub-plots, and diameter at breast height threshold of 10 cm. A smaller efficiency score indicates greater efficiency. AGB = above-ground biomass, USD = U.S. dollars, BAF = basal area factor, VBAR = volume to basal area ratio, $dist_{SP}$ = distance from subplots to center, r_{max} = truncated maximum distance of tree inclusion.

Configuration	Number of plots	Number of trees	Mean AGB (Mg ha $^{-1}$)	Standard error of AGB (Mg ha $^{-1}$)	Total time cost range USD	Efficiency
FP: 0.1 ha 10+ cm	4	493	148	32.1	\$950 \$2059	0.98 2.12
NP: 0.1 ha 30+ cm 0.025 ha 10+ cm	4	463	137	32.0	\$1025 \$2066	1.05 2.11
AC cluster plot of 4 sub-plots TC, BAF = 3 VBAR, BAF = 12 $dist_{SP}$ = 12.6 m r_{max} = 17.8 m	4	325 (TC diameter), 163 (VBAR diameter, height)	126	21.4	\$578 \$946	0.27 0.43

Results

Measurements for cost estimates

Travel and measurement times were recorded on the OTS-Costa Rica site and are presented in Table 4. These cost estimates are employed in calculating the efficiency metrics together with the precision estimates for the OTS-Costa Rica site as shown in the next section (Table 5). The unit costs from the OTS-Costa Rica site are also applied to the estimates based on sampling simulation with the BCI-Panama data and are provided in the next sections. The times and costs consist of (i) traveling (to the first plot from the closest point of the border of site, between the plots and returning to the border of the site), (ii) plot establishment, and (iii) tree measurements. Table 4 shows the travel speeds and times needed for plot establishment and tree measurements along with the unit costs.

In the OTS-Costa Rica site, traveling contributed <1% and plot establishment <5% to the total field time costs with the remainder dominated by tree measurement time. Travel costs depend naturally on the size of the inventory site, the number of plots and the plot layout, that is, sampling design. We also used these travel speed and measurement time estimates with the BCI-Panama site data for sampling simulation, assuming that the cost components are similar at both sites. Tree measurement was also the most expensive component at the BCI-Panama site across all plot configurations simulated.

Estimates and error estimates based on field measurements on the OTS site in Costa Rica

Table 5 shows the AGB estimates and sampling error estimates based on the field measurements in the OTS-Costa Rica site. The three plot configurations are fixed-area circular plot (size 0.1 ha), nested plots (sizes 0.1 and 0.025 ha with 30-cm dbh threshold) and a cluster of angle-count plots (BAF 3). The standard errors of the AGB estimates are close to each other for the fixed-area plots and nested plots but smaller for the angle-count cluster plot. The sampling errors of the estimates of the different configurations do not deviate statistically significantly (even at 10% significance level) due to small sample sizes. However, the results are consistent with the results in the BCI-Panama site, see the following section.

Estimates and error estimates based on sampling simulation with Barro Colorado data

Tables 6 and 7 show the estimates and sampling error estimates (Eqs. 5 and 6) for AGB and G together with the average numbers of

Table 6. Sampling error, measurement cost and efficiency of alterative fixed-area plot (FP) and nested plot (NP) configurations simulated using data from Barro Colorado Island, Panama. Trees with diameter at breast height (dbh) ≥10 cm are included; number of plots is 32. A smaller efficiency score indicates greater efficiency. G = basal area, AGB = above-ground biomass, USD = U.S. dollars.

Plot configuration, dbh thresholds, cm	Area, ha	No of trees measured	Mean G, m^2 ha^{-1}	Sampling error	Mean AGB, Mg ha^{-1}	Sampling error	Total costs, USD	Efficiency
FP	0.1	1304	27.51	1.94	289.75	19.67	$6717	0.260
FP	0.05	646	26.16	2.07	272.92	22.25	$4249	0.210
NP	0.05	776	27.45	2.01	289.27	20.51	$5697	0.240
10, 30	0.1							
NP	0.0250	515	27.39	1.95	289.00	20.23	$4719	0.193
10, 30	0.1							
NP	0.025	431	27.16	2.17	286.55	22.19	$4405	0.217
10, 40	0.1							
NP	0.0125	290	27.13	2.51	286.60	25.21	$3876	0.246
10, 40	0.1							
NP	0.0125	237	27.52	2.90	291.20	29.38	$3676	0.317
10, 50	0.1							
NP	0.0125	325	27.77	2.38	294.58	23.42	$4005	0.220
10, 50	0.2							

Table 7. Sampling error, measurement cost, and efficiency of alterative angle-count (AC) plot configurations simulated using data from Barro Colorado Island, Panama. Trees with diameter at breast height (dbh) ≥10 cm are included; number of plots is 32. Both single plots and clusters of sub-plots were tested. FP = fixed-area plot, BAF = basal area factor, G = basal area, ABG = above-ground biomass, USD = U.S. dollars, $dist_{SP}$ = distance from subplots to center, r_{max} = truncated maximum distance of tree inclusion, r = FP radius.

Plot configuration, dbh thresholds (cm) and the radius of FP	BAF	Trees measured	Mean G, m^2 ha^{-1}	Sampling error	Mean AGB, Mg ha^{-1}	Sampling error	Total cost USD	Efficiency
AC	2	423	27.17	1.20	287.57	12.51	$2690	0.042
AC	3	285	27.43	1.52	289.74	13.30	$1964	0.035
AC, r_{max} = 25.2 m	3	249	27.60	2.04	291.8	19.62	$1775	0.068
AC, r_{max} = 17.8 m	3	219	27.32	2.36	288.4	23.44	$1617	0.089
AC	4	213	27.21	1.80	287.44	17.00	$1586	0.046
AC	5	170	27.19	2.15	287.91	19.29	$1360	0.051
AC	8	107	27.33	2.63	289.46	23.41	$1029	0.056
AC	10	85	27.29	2.96	289.16	27.88	$914	0.071
AC	12	71	27.27	3.25	289.53	34.13	$840	0.098
AC cluster plot of 4 sub-plots $dist_{SP}$ = 12.6 m	12	252	28.00	2.10	293.77	20.20	$2190	0.089
r_{max} = 12.6 m								
AC cluster plot of 4 sub-plots $dist_{SP}$ = 20 m r_{max} = 20 m	12	275	27.6	1.77	290.34	18.08	$2311	0.076
AC cluster plot of 4 sub-plots $dist_{SP}$ = 20 m r_{max} = 20 m	16	211	27.63	1.98	291.36	20.57	$1973	0.083
AC cluster plot of 4 sub-plots $dist_{SP}$ = 20 m r_{max} = 20 m	20	170	27.58	2.29	291.06	23.32	$1762	0.096
FP r = 5 m 10 ≤dbh <17.32 AC, dbh ≥ 17.32 cm	3	311	27.46	1.44	290.03	13.05	$2498	0.043

trees over the samples, average total measurement costs and the efficiency metrics (Eq. 7 with $c = 10^7$) for selected plot configurations. Only trees with a dbh greater than or equal to 10 cm were included following the practice in the field in the OTS-Costa Rica site. These trees comprise 87% of the basal area and 95% of the total AGB of all trees on the study site (Table 1).

The plot configurations shown in the tables are fixed-area circular plots, nested circular plots (both in Table 6) and angle-count plots (Table 7).

Fixed-area plots and nested plots

As expected, fixed-area plots included a large number of small trees and were thus expensive to measure. Furthermore, the sampling errors were relatively large. Two examples are shown in Table 6 with areas of 0.1 ha and 0.05 ha (the radii ~17.84 and 12.62 m).

With nested plots, the area of the smaller circle was either 0.05, 0.025 or 0.0125 ha (radius ~12.62, 8.92, or 6.31 m) and the area of the larger circle was 0.1 ha (radius 17.84 m) except in one case in which it was 0.2 ha (radius 25.23 m). The dbh threshold for the trees included for the larger circle was either 30, 40, or 50 cm. These thresholds were selected looking at the distributions of AGB and G by dbh categories in the population (Table 2). The relative sampling errors for both G and AGB were <10% except for the small 0.0125-ha and large 0.1-ha plots with a dbh threshold of 50 cm. Increasing the area of the large plot to 0.2 ha decreased error but also increased cost. The nested plot configuration with a plot size of 0.025 ha for trees with dhh smaller than or equal to 30 cm and 0.1 ha for the other trees had the smallest (best) efficiency metric (0.193) but was still much larger than those for the most efficient angle-count plots (0.041) (Tables 6 and 7). These results confirm that a cost-efficient inventory could be achieved by measuring small-diameter trees on small plots only, and sparsely distributed large-diameter trees on large plots. This principle can be realized using PPS sampling, e.g. angle-count sampling.

Angle-count plots

The BAFs with angle-count plots varied from 2 to 12, with additional tests of 16 and 20. Some angle-count plots were tested with

Table 8. Examples of plot configurations and the number of plots needed to meet ±10% relative sampling error at 90% confidence interval for basal area (G) and above-ground biomass (AGB) estimates together with the expected number of trees. Data from Barro Colorado Island, Panama are used for simulations. Note that the standard error of G is 1.67 m^2ha^{-1} and that of AGB is 17.70 Mg ha^{-1}. 4 × AC = AC cluster plot of 4 sub-plots, $dist_{SP}$ = distance from subplots to center, r_{max} = truncated maximum distance of tree inclusion, SD = standard deviation.

Plot configuration area, dbh thresholds	G				AGB				
	No of plots needed	Expected number of trees	Sample mean (m^2ha^{-1})	Sample SD (m^2ha^{-1})	No of plots needed	Expected number of trees	Sample mean (Mg ha^{-1})	Sample SD (Mg ha^{-})	Total cost USD
FP, 0.1 ha	41	1650	27.51	10.62	62	2509	289.75	138.86	$12 844
FP, 0.05 ha	66	1331	26.16	13.55	105	2127	272.98	181.71	$13 796
NP, 0.025 ha, dbh < 40 cm	44	598	27.16	11.12	65	873	286.55	142.42	$8832
NP, 0.0125 ha, dbh < 40 cm	51	460	27.13	11.89	69	629	286.60	147.29	$8294
NP, 0.0125 ha, dbh < 50 cm	47	475	27.77	11.41	60	613	294.58	137.54	$7486
FP, 5 m (0.0008 ha) + AC, BAF = 3	24	232	27.43	8.18	34	325	289.84	102.76	$2205
AC, BAF = 3	28	246	27.43	8.76	33	3101	289.74	104.45	$2146
AC, BAF = 3, r_{max} = 25.2	36	281	27.59	10.03	46	359	291.78	120.26	$2513
AC, BAF = 3, r_{max} = 17.8	53	360	27.32	12.11	50	476	288.39	147.55	$3179
AC, BAF = 3, r_{max} = 12.6	77	429	25.97	14.62	111	619	271.61	186.12	$4696
AC, BAF = 4	35	231	27.21	9.84	43	285	287.44	116.00	$2107
AC, BAF = 5	42	226	27.19	10.87	50	268	287.91	125.61	$2088
AC, BAF = 8	70	232	27.33	13.91	80	266	289.46	157.84	$2410
AC, BAF = 10	91	241	7.29	15.86	102	273	289.16	178.82	$2736
AC, BAF = 12	107	238	27.27	17.27	123	274	289.53	196.51	$2996
4 × AC, BAF = 12 $dist_{SP}$ = 12.6 m r_{max} = 12.6 m	45	357	27.99	11.25	54	428	293.78	130.59	$3650
4 × AC, BAF = 12 $dist_{SP}$ = 20 m r_{max} = 20 m	30	258	27.56	9.14	34	291	290.34	103.05	$2452

Table 9. Total costs broken into components to meet a relative sampling error of ±10% at 90% confidence interval. Plot configurations are selected from Table 8. Net present value (NPV) of the total cost is calculated assuming measurements every 5 years over a 50-year period; costs are discounted to the present at 5%. USD = U.S. dollars, FP = fixed-area plot, NP = nested plot, 4 × AC = angle-count plot of four sub-plots, dbh = diameter at breast height, $dist_{SP}$ = distance from subplots to center, r_{max} = truncated maximum distance of tree inclusion, r = radius of FP, BAF = basal area factor.

Plot configuration	Travel cost	Establishment cost	Measurement cost	Total cost	Total cost ha^{-1} USD	Total cost per CO_2e Mg	NPV USD
FP, 0.1 ha	$206	$3232	$9407	$12 845	$257	$0.48	$55 281
FP, 0.05 ha	$284	$5535	$7977	13 796	$276	$0.52	$59 375
NP 0.025 ha dbh < 40 cm	$215	$5344	$3274	$8832	$177	$0.33	$38 013
NP, 0.0125 ha dbh < 40 cm	$223	$5715	$2357	$8294	$166	$0.31	$35 698
NP, 0.0125 ha dbh < 50 cm	$202	$4983	$2298	$7483	$150	$0.28	$32 205
FP, r = 5 m (0.0008 ha) + AC, BAF = 3	$157	$340	$1709	$2205	$44	$0.08	$9491
AC, BAF = 3	$161	$350	$1631	$2142	$43	$0.08	$9218
4 × AC, BAF = 12, $dist_{SP}$ = 20 mr_{max} = 20 m	$157	$765	$1530	$2452	$49	$0.09	$10 551

a maximum distance to the trees included, that is, a truncated angle-count plot was used (Table 7). The inclusion probability in this case is given in Eq. 4. Decreasing the BAF naturally decreased the sampling errors of AGB and G but the increase in the number of trees measured began to decrease the efficiency when the BAF was smaller than 3. The relative sampling errors for AGB with the BAF values of 16 and 20 were large, 15.4% and 17.4% respectively (not shown in Table 7).

Truncation of the angle-plot increased sampling errors with BAF = 3, indicating that large trees are important in AGB and G estimation. The similar effect could be seen when using BAF = 5 instead of BAF = 3 and a maximum distance of 25.2 m. The errors were about the same, but the number of trees measured was smaller for BAF = 5.

An interesting alternative was a small fixed-area plot for trees with a small dbh in conjunction with angle-count sampling for trees larger than the dbh threshold. Table 7 shows an example in which the radius of a fixed-area plot is 5 m for the trees 10 cm ≤ dbh < 17.32 cm and the BAF of the angle-count plot = 3. Another interesting alternative is a cluster of four angle-count sub-plots with a large BAF. The results with the BAF values of 12, 16, and 20 are shown in Table 7. The distance of the sub-plots from the center of the configuration was either 12.6 m or 20 m for BAF 12, and 20 m for BAF 16 and 20. The maximum distance from the center of the sub-plot to the trees in the sub-plots was the same as the distances of the centers of the sub-plots to the center of the plot configuration, so that the sub-plots did not overlap. The efficiencies of those clusters of sub-plots with the criteria used were better than those of the fixed-area and nested plots and close to those of some single angle-count plots.

As a conclusion, angle-count sampling turned out to be a cost-efficient alternative to fixed-area and nested plots. The sampling errors depend on the number of plots and the area of the study site, and naturally on the variance of the characteristics in question. A BAF of 8 to 10 is small enough to achieve a relative sampling error of ∼10% with 32 plots at the BCI-Panama site.

Estimating plot numbers for precision targets

Another way to evaluate the alternative plot configurations was to estimate the number of plots needed to meet a given relative sampling error, here 10%, with a given confidence interval, here 90% (Eq. 11). Table 8 shows the results for G and AGB for some plot configurations selected from Tables 6 and 7. In addition to numbers of plots, the expected numbers of trees are also shown together with the estimated sample means and sample standard deviations of the plot-level characteristics. Total costs for the AGB estimates for those configurations, and the number of plots and trees obtained, are also shown. Data from the BCI-Panama site and sampling simulation were used. Note that these calculations assume random locations of the plots, not, e.g. the systematic locations as in the calculations in Tables 6 and 7.

The variations of the numbers of plots needed to meet our target sampling error for G and AGB were similar. The smallest number of plots, 33, for AGB estimation with the criterion used was achieved with the angle-count plot with a BAF of 3. The number of the plots was almost the same, 34, for the plot configurations of a small fixed-area plot combined with an angle-count plot (BAF = 3), and also for the cluster of 4 sub-plots with a BAF of 12.

The numbers of plots needed was larger for angle-count plots with a BAF of 8, 10, and 12 than for plots with a smaller BAF and, also, e.g. for the fixed-area plot with the size of 0.1 ha. The smaller number of trees to be measured on angle-count plots with a larger BAF, and particularly compared to fixed-area or nested plots, make this configuration competitive when using this criterion. The fixed-area plots and nested plots were noticeably more expensive than the cheapest plot alternatives (i.e. the angle-count plots with a BAF of 3, 4, 5, and 8), with costs of 2100–2400 USD.

The alternative of a cluster of sub-plots also worked well with this criterion. The costs of a cluster of four angle-count sub-plots with a BAF of 12 and maximum distance of 20 m were near the costs of the cheapest one, 2452 USD.

A reduction of the maximum distance increased the costs of the cluster due to the larger numbers of plots and trees needed to meet the precision requirements. This criterion also confirmed the advantage of the angle-count plots, particularly with large BAFs (even with a BAF = 12 when a cluster of sub-plots are used).

Summarizing the cost and efficiency results in Tables 6 and 7, the costs and efficiencies of the fixed-area and nested plots with 32 plots varied between 3700 and 6700 USD and the efficiency metric between 0.19 and 0.32. The angle-count plots and their many variants with the same number of the plots had costs between 840 and 2700 USD and efficiency values between 0.035 and 0.098. Recall that the efficiency metric takes into account the error estimates in addition to estimated costs.

Table 9 shows the costs broken down into components for selected plot configurations using the precision criterion mentioned above. The table also presents the cost per hectare, the cost per CO_2e, and the net present value (NPV) at a 5% interest rate of the costs of AGB inventories taken every 5 years over a 50-year period for a potential avoided deforestation FCO project. The NPV values were discounted and calculated using Eq 8. The NPV for the angle-count plots is ∼9200–10 500 USD, while the NPVs for the nested plots range from 32 000–38 000 USD, and those for fixed-area plots range from 55 000–59 000 USD.

Discussion

The costs of the alternative plot configurations varied significantly given the same number of plots and roughly the same precision metrics. The costs of the circular fixed-area plot (0.1 ha) were the highest among the alternatives tested for estimating AGB. The costs were almost twice those of the nested plot alternatives and 6–7 times the costs of angle-count plots, yet the sampling errors were nearly equivalent among all of these configurations when compared to the costs of the designs with 32 plots and the BCI-Panama site data. The smaller fixed-area plot (0.05 ha) nearly halved the costs compared to the larger fixed-area plot, while increasing the sampling error by only ∼13%. This preference for smaller plot areas, within bounds, is consistent with previous theoretical treatments that take into account cost as well as variance (Lynch 2017).

Among the nested plot alternatives, the plots with sizes of 0.2 ha for trees with dbh ≥ 50 cm and 0.0125 ha for smaller trees proved to be the most efficient based on the efficiency criterion (Table 6). Reducing the size of the larger plot to 0.1 ha reduced the costs but also increased sampling errors. The nested plot design with a 50 cm dbh threshold was promoted by the United States Agency for International Development (USAID) for AGB measurement in tropical forests through its Lowering Emissions in Asian Forests initiative in 2011–2016 (Winrock International 2025). Our findings regarding nested plots are consistent with these recommendations.

The costs of angle-count plots remained much lower than those of the cheapest nested plots in our study, without significantly increasing errors up to a BAF of 8: 800–1600 USD, compared to the 3700–4400 USD of the most competitive nested plots.

The criterion of the number of plots and trees required to achieve an AGB sampling error of no >10% with a 90% confidence interval further highlighted the superior performance of the angle-count plots in the present study. The lowest costs were achieved with BAF values of 3, 4, 5, and 8 (ranging from 2100 to 2400 USD), compared to >13 000 USD for fixed-area plots and over 7500 USD for nested plots. Restricting the maximum distance to the trees included in the plot (using truncated angle-count plots) increased the number of plots needed with a BAF of 3 by 30% and the numbers of trees measured by 38%. Larger values of BAF and a cluster of angle-count sub-plots turned out to be a very competitive alternative. The reason for the small increase of the costs in this case is the need to increase the number of plots to reach the precision criteria for the AGB estimates. The sparsely populated large trees contribute heavily to both the mean and variance of AGB estimates.

Truncated angle-count plots were used for the first time in the Finnish NFI in NFI8 (1986–2003) in the early 1990s in North Finland, and in the entire country in NFI9 (1996–2004) (Tomppo et al. 2001, 2011). The motivation for this was to reduce costs without increasing sampling errors, while reducing the bias that may be caused by unobserved trees. The performance of the truncated plots was also studied by Berger et al. (2020) in the context of the Austrian NFI. In that case, truncation led to a larger stock estimate because fewer trees were missed. It also caused greater uncertainty of the estimates relative to the Finnish NFI. This uncertainty may be due to greater variation in diameter distributions and tree densities in Austrian versus Finnish forests.

Clusters of four sub-plots with a BAF of 12, and also with 16 and 20, worked very well with regard to our criteria, particularly with a maximum distance of 20 m; these were nearly as efficient as the single angle-count plot without restrictions (BAF values 4 and 5). A hybrid plot combining a small fixed-area plot and an angle-count plot for trees outside the fixed-area circle also showed relatively low costs with small sampling errors. When a cluster of angle-count sub-plots is used, particularly without truncation, a single large-diameter tree could fall within the angle of inclusion of multiple sub-plots. Van Deusen and Grender (1989) presented an alternative estimator for angle-count cluster plots for the case where the sub-plots overlap. The purpose of the method and estimator was to reduce the variance of the estimators without changing the sampling design. Our results show that clusters of angle-count plots are very competitive, even when ordinary estimating equations are used; if alternatives further reduce the variance, the efficiency would be further improved.

The performance of angle-count plots, particularly with large BAFs, has been rarely studied in tropical inventories. In temperate forests, Marshall et al. (2004) used (relatively) large BAFs for volume estimation. In two stands, BAFs as large as 20.66 and 57.59 m^2ha^{-1} were used for sub-sampling. The "big BAF method" in selecting the trees for volume to basal area ratio estimation made the inventory more statistically efficient. The average volumes and densities of large trees were larger than in our BCI-Panama site. Clusters of sub-plots in angle-count plots have been studied even less than the basic angle-count plots.

The BAFs employed with angle-count sampling and plots, and commonly used in practical inventories, are smaller than the largest ones used here. Austrian and German NFIs use a BAF of 4 (Gschwantner et al. 2010, Polley et al. 2010). The Finnish NFI used 1.5 in North Finland and 2 in the southern part of the country (Tomppo et al. 2001, 2011). In complex forests of eastern North America, BAFs from 2.3 to 4.6 are common, though BAFs at the larger end of this range are most often recommended both for point and line sampling (Wensel et al. 1980, Wiant Jr et al. 1984, Ducey 2001, Ducey et al. 2002). The good performance of large BAFs in tropical forests is caused by the heavily right-skewed diameter distribution: a large density of small diameter trees and small density of very large trees that drive basal area, biomass, and volume.

Overall, angle-count methodology, originally designed by Bitterlich (1948) for efficient estimation of timber volume in European forests through direct measurement of basal area, tightly correlate with timber volume and has proven to be efficient. In addition, its underlying principle, PPS sampling, has proven to be efficient in estimating other forest parameters, including those related to tropical forests. One further advantage of angle-count sampling is that a large BAF can be used in selecting a sub-sample of trees, e.g. for height measurements and for constructing height-diameter models, when height measurements are time-consuming and costly, as typically the case in the tropics.

Employing remote sensing together with ground measurement can also make inventories more cost-efficient than those using ground measurements only. A cluster of sub-plots could be used as training data in multiple ways (e.g. Tomppo et al. 2014, Palace et al. 2015, Fassnacht et al. 2024), particularly when using multi-resolution remote sensing and multi-source inventory (McRoberts and Tomppo 2007, Coops et al. 2023) However, when considering the use of remote sensing in the tropics, one should keep in mind the challenging conditions with highly diverse forests including large numbers of tree species, and also the benefits of spatially explicit field data for calibration. Angle-count plots may present further challenges with these applications, depending on how auxiliary data are used. Stratification (pre and post) is not as sensitive to the quality of the remote sensing-aided estimates as the model-based approach is.

Additional considerations

We focus on circular plots and their variations only, including angle-count plots, in this study. Other alternatives include square and rectangular plots, often employed in the tropics. There are also other methods to assess the cost-efficiency than the simple methods that we used, as well as methods for multi-purpose inventory (da Silva et al. 2003, Baraloto et al. 2012, Netto et al. 2014, Henttonen and Kangas 2015, Pinto et al. 2021).

It should also be noted that our focus was on AGB and G for FCO projects. For other characteristics, such as tree density and species composition, forest management, biodiversity conservation, non-timber forest products, and cultural values, fixed-area plots or other more complex plot configurations may be more favorable. Our hybrid plot design, combining a fixed-area plot and an angle-count plot, could offer a partial solution for such cases. Additional studies are needed to answer all of these questions.

When assessing costs, it is important to note that the same cost rates were applied to both small and large trees. Using tree-size-specific costs could alter the conclusions to some extent. We also acknowledge the problem of ingrowth related to the use of angle-count plots for increment estimation at permanent locations and are currently testing distance variable equations in the field (McTague et al. 2010) to address this problem.

Our results are based on the analyses in two specific study sites of wet tropical forests. The parameter of an efficient plot configuration depends, in addition to the variables of interest, also on the structure of the forests of interest. The methods presented here could possibly be utilized in the analyses and decision making in other applications.

One should also note that the number of the plots and the measurement costs needed to meet the used precision requirement were estimated for an area of 50 ha. The number of the plots and costs do not increase proportionally to the size of the area. The cost per ha (Table 9) decreases when the area of interest increases assuming that there is not significant variation in forests in the area of interest, or trend-like changes in the forest variables.

Conclusion

Alternative ground-based plot configurations were compared to assess the precision of above-ground biomass and basal area estimates, as well as measurement costs, using two study sites in tropical forests. Key findings include:

- Angle-count plots emerged as a highly cost-efficient plot configuration for forest inventories in tropical regions with high tree density and size variability.
- Large BAFs (3–8) can be used to achieve low sampling errors (∼10%) with fewer plots and trees.

- Clustered large-BAF angle-count subplots (e.g. BAF = 12, 16, or 20) are a promising alternative to increase efficiency and merit further study, also with alternative error estimates.
- Small fixed-area plots for small trees can be combined with angle-count plots for larger trees and is a worthwhile option for further investigation, particularly if stem count is of interest.

These findings highlight the adaptability and efficiency of angle-count sampling for addressing above-ground tree biomass inventory needs and diverse sampling requirements.

Acknowledgments

The authors thank the Editor-in-Chief, Prof. Dr. Fabian Faßnacht and the three anonymous reviewers for their valuable comments and recommendations on the two earlier versions of the manuscript. The comments have improved the manuscript significantly. The authors acknowledge R. Condit for provision of historical data from STRI BCI Panama for simulations and D. and D. Clark for access to Carbono plots at La Selva Costa Rica for field inventory. L. Campos and W. Miranda provided field support. K. Iles and D. Wang provided useful comments on an earlier version of this manuscript.

Author contributions

Erkki Tomppo (Conceptualization, Data curation, Formal analysis, Investigation, Methodology, Project administration, Software, Validation, Visualization, Writing—original draft, Writing—review & editing), Bryan Conrad Foster (Conceptualization, Data curation, Funding acquisition, Investigation, Methodology, Resources, Writing—original draft, Writing—review & editing), Laura S Kenefic (Conceptualization, Investigation, Methodology, Resources, Supervision, Writing—original draft, Writing—review & editing), and Mark J. Ducey (Conceptualization, Investigation, Methodology, Resources, Supervision, Validation, Writing—original draft, Writing—review & editing)

Supplementary material

Supplementary material are available at *Forestry* online.

Conflict of interest: None declared.

Funding

Funding was provided by the New Hampshire Agricultural Experiment Station, USDA National Institute of Food and McIntire-Stennis Project 1022727, and by Foster Forestry and Environmental Consulting LLC.

Data availability

By request. R code and instructions available by request from the corresponding author.

References

Achard F, Boschetti L, Brown S. *et al.* *GOFC-GOLD: A sourcebook of methods and procedures for monitoring and reporting anthropogenic GHG emissions and removals associated with deforestation*. In: *Gains and Losses of Carbon Stocks in Forests Remaining Forests, and Forestation. Version COP22–1*. GOFC-GOLD Land Cover Project Office. Wageningen University, Amsterdam, Netherlands, 2014, 255 p.

Ali A, Lin S-L, He J-K. *et al.* Big-sized trees overrule remaining trees' attributes and species richness as determinants of aboveground biomass in tropical forests. *Glob Chang Bio* 2019;**25**:2810–24. https://doi.org/10.1111/gcb.14707.

Alijanpour A, Jabbari K, Eshaghi RJ. *et al.* Comparing performance of fixed and variable area sampling plots in Iranian sub-humid forests. *Appl Ecol Environ Res* 2018;**16**:2815–25. https://doi.org/10.15666/aeer/1603_28152825.

Banyard SG. A comparison between point sampling and plot sampling in tropical rain forests based on a concept of the equivalent relascope plot size. *Commonwealth For Rev* 1975;**54**:312–20 http://www.jstor.com/stable/42604450.

Baraloto C, Molto Q, Rabaud S. *et al.* Rapid simultaneous estimation of aboveground biomass and tree diversity across neotropical forests: A comparison of field inventory methods. *Biotrop.* 2012;**45**: 288–98. https://doi.org/10.1111/btp.12006.

Bastin J-F, Rutishauser E, Kellner JR. *et al.* Pan tropical prediction of forest structure from the largest trees. *Glob Ecol Biogeog* 2018;**27**: 1366–83. https://doi.org/10.1111/geb.12803.

Berger A, Gschwantner T, Schadauer K. The effects of truncating the angle count sampling method on the Austrian National Forest Inventory. *Ann Sci* 2020;**77**:1–11. https://doi.org/10.1007/s13595-019-0907-y.

Bitterlich W. *Die Winkelzählprobe. Allg. Forst-Holzwirtsch. Ztg*, Vol. **59**, 1948, 4–5.

Chave J, Condit R, Lao S. *et al.* Spatial and temporal variation of biomass in a tropical forest: Results from a large census plot in Panama. *J Eco* 2003;**91**:240–52. https://doi.org/10.1046/j.1365-2745.2003.00757.x.

Chave J, Réjou-Méchain M, Búrquez A. *et al.* Improved allometric models to estimate the aboveground biomass of tropical trees. *Glob Chang Bio* 2014;**20**:3177–90. https://doi.org/10.1111/gcb.12629.

Clark DB, Clark DA. Landscape-scale variation in forest structure and biomass in a tropical rain forest. *For Ecol Manage* 2000;**137**:185–98. https://doi.org/10.1016/S0378-1127(99)00327-8.

Clark DA, Clark DB. Assessing tropical forests' climate sensitivities with long-term data. *Biotrop* 2011;**43**:31–40. https://doi.org/10.1111/j.1744-7429.2010.00654.x.

Clark D, Clark D. Two decades of annual landscape-scale tree growth and dynamics in old-growth tropical rainforest in the CARBONO project, La Selva Biological Station, 1997-2018 [dataset]. *Dryad* 2021. https://doi.org/10.5061/dryad.51c59zw8n.

Clark DB, Ferraz A, Clark DA. *et al.* Diversity, distribution and dynamics of large trees across an old-growth lowland tropical rain forest landscape. *PloS One* 2019;**14**:e0224896. https://doi.org/10.1371/journal.pone.0224896.

Condit R. *Tropical Forest Census Plots: Methods and Results from Barro Colorado Island, Panama and a Comparison with Other Plots*. Berlin, Germany: Springer-Verlag, 1998, 211.

Condit R, Perez R, Aguilar S. *et al.* *Complete Data from the Barro Colorado 50-ha Plot: 423617 Trees, 35 Years, 2019 Version*. Washington, D.C.: Smithsonian Tropical Research Institute, 2019. https://doi.org/10.15146/5xcp-0d46.

Coops NC, Tompalski P, Goodbody TRH. *et al.* Framework for near real-time forest inventory using multi source remote sensing data. *Forestry* 2023;**96**:1–19. https://doi.org/10.1093/forestry/cpac015.

Cressie N, Hawkins DM. Robust estimation of the variogram. *J Internat Assoc Mathemat Geol* 1980;**12**:115–25. https://doi.org/10.1007/BF01035243.

Cushman KC, Bunyavejchewin S, Cardenas D. *et al.* Variation in trunk taper of buttressed trees within and among five lowland tropical forests. *Biotrop* 2021a;**53**:1442–53. https://doi.org/10.1111/btp.12994.

Cushman KC, Burley JT, Imbach B. *et al.* Impact of a tropical forest blowdown on aboveground carbon balance. *Sci Rep* 2021b;**11**:11279. https://doi.org/10.1038/s41598-021-90576-x.

da Silva RL, Xavier A, Leite HG. *et al.* Determination of the experimental optimum plot size by maximum modified curvation, intraclass correlation coefficient and visual analysis methods in eucalypt clonal tests. *Revista Árvore* 2003;**27**:669–76. https://doi.org/https://doi.org/10.1590/S0100-67622003000500009.

Druszcz JP, Nakajima NY, Netto SP. *et al.* Comparison between Bitterlich and fixed area circular plot sampling methods in Pinus taeda L plantation. *Floresta* 2010;**40**:739–54. https://doi.org/10.5380/rf.v40i4.20326.

Ducey MJ. Pre-cruise planning. In: Bennett K, (ed.). *Workshop Proceedings: Forest Measurements for Natural Resource Professionals*. Cooperative Extension, Durham, New Hampshire: University of New Hampshire, 2001, 26–35.

Ducey MJ. Sampling trees with probability nearly proportional to biomass. *For Ecol Manage* 2009;**258**:2110–6. https://doi.org/10.1016/j.foreco.2009.08.008.

Ducey MJ, Jordan GJ, Gove JH. *et al.* A practical modification of horizontal line sampling for snag and cavity tree inventory. *Can J For Res* 2002;**32**:1217–24. https://doi.org/10.1139/x02-038.

Fassnacht FE, White JC, Wulder MA. *et al.* Remote sensing in forestry: Current challenges, considerations and directions. *Forestry* 2024;**97**:11–37. https://doi.org/10.1093/forestry/cpad024.

Feldpausch TR, Lloyd J, Lewis SL. *et al.* Tree height integrated into pantropical forest biomass estimates. *Biosci.* 2012;**9**:3381–403. https://doi.org/10.5194/bg-9-3381-2012.

Fichtler E, Clark DA, Worbes M. Age and long-term growth of trees in an old-growth tropical rain forest based on analyses of trees rings and 14-C. *Biotrop* 2003;**35**:306–17. https://doi.org/10.1111/j.1744-7429.2003.tb00585.x.

Forest Carbon Offsets. 2023. Everything you need to know. Available here: https://carboncredits.com/forest-carbon-offsets-everything-you-need-to-know/

ForestGeo. 2025. Available here: https://forestgeo.si.edu/.

Foster BC, Wang D, Auld G. *et al.* Assessing audit impact and thoroughness of VCS forest carbon offset projects. *Environ Sci Policy* 2017;**78**:121–41. https://doi.org/10.1016/j.envsci.2017.09.010.

Gregoire TG. Design-based and model-based inference in survey sampling: Appreciating the difference. *Can J For Res* 1998;**28**:1429–47. https://doi.org/10.1139/x98-166.

Gregoire TG, Valentine HT. *Sampling Strategies for Natural Resources and the Environment*. New York: Chapman and Hall, 2007, 496. https://doi.org/10.1201/9780203498880.

Griscom BW, Adams J, Ellis PW. *et al.* Natural climate solutions. *Proc Natl Acad Sci* 2017;**114**:11645–50. https://doi.org/10.1073/pnas.1710465114.

Grosenbaugh LR, Stover WF. Point sampling compared with plot sampling in Southeast Texas. *For Sci* 1957;**3**:2–14. https://doi.org/10.1093/forestscience/3.1.2.

Gschwantner T, Gabler K, Schadauer K. *et al.* In: Tomppo E, Gschwantner T, Lawrence M. *et al.*, (eds.). *Individual Country Reports: Austria. In: National Forest Inventories - Pathways for Common Reporting*. New York: Springer, 2010, 612. https://doi.org/10.1007/978-90-481-3233-1.

Hardiman BS, Gough CM, Halperin A. *et al.* Maintaining high rates of carbon storage in old forests: A mechanism linking canopy structure to forest function. *For Eco Manage* 2013;**298**:111–9. https://doi.org/10.1016/j.foreco.2013.02.031.

Harris NL, Gibbs DA, Baccini A. *et al.* Global maps of twenty-first century forest carbon fluxes. *Nat Clim Chang* 2021;**11**:234–40. https://doi.org/10.1038/s41558-020-00976-6.

Henttonen HM, Kangas A. Optimal plot design in a multipurpose forest inventory. *For Ecosys* 2015;**2**:31. https://doi.org/10.1186/s40663-015-0055-2.

Holdaway R, McNeill SJ, Mason NWH. *et al.* Propagating uncertainty in plot-based estimates of forest carbon stock and stock change. *Ecosys* 2014;**17**:627–40. https://doi.org/10.1007/s10021-014-9749-5.

Horvitz DG, Thompson DJ. A generalization of sampling without replacement from a finite universe. *J Amer Stat Assoc* 1952;**47**:663–85. https://doi.org/10.1080/01621459.1952.10483446.

Hunter MO, Keller M, Vitoria D. *et al.* Tree height and tropical forest biomass estimation. *Biogeosci* 2013;**10**:8385–99. https://doi.org/10.5194/bg-10-8385-2013.

Iles K, Fall M. Can an angle gauge really evaluate "borderline trees" accurately in variable plot sampling? *Can J For Res* 1988;**18**:781 https://cdnsciencepub.com/doi/abs/10.1139/x88-118.

Kershaw JA Jr, Ducey MJ, Beers TW. *et al. Forest Mensuration*. 5th edition. Hoboken, New Jersey: Wiley-Blackwell, 2016, 640. https://doi.org/10.1002/9781118902028.

Kricher, JC. Rain Forest: The Realm of the Plants. In *The New Neotropical Companion*. Princeton University Press, 2017, 39–57. https://doi.org/10.1515/9781400885589-006.

Larjavaara M, Muller-Landau H. Measuring tree height: A quantitative comparison of two common field methods in a moist tropical forest. *Meth Ecol Evol* 2013;**4**:793–801. https://doi.org/10.1111/2041-210X.12071.

Leigh EGJ. *Tropical Forest Ecology: A View from Barro Colorado Island*. New York: Oxford University Press, 1999, 245.

Lionjanga DL, Pereira E. Comparación de los métodos de muestreo casual simples: Bitterlich y Prodan. *Revista Forestal Baracoa* 2014;**33**:76–86.

Lister AJ, Leites LP. Cost implications of cluster plot design choices for precise estimation of forest attributes in landscapes and forests of varying heterogeneity. *Can J For Res* 2022;**52**:188–200. https://doi.org/10.1139/cjfr-2020-0509.

Lutz JA, Furniss TJ, Johnson DJ. *et al.* Global importance of large diameter trees. *Glo Ecol Biogeo* 2018;**27**:849–64. https://doi.org/10.1111/geb.12747.

Lynch TB. Optimal sample size and plot size or point sampling factor based on cost-plus-loss using the Fairfield smith relationship for plot size. *Forestry* 2017;**90**:697–709. https://doi.org/10.1093/forestry/cpx024.

Marshall DD, Iles K, Bell JF. Using a large-angle gauge to select trees for measurement in variable plot sampling. *Can J For Res* 2004;**34**:840–5. https://doi.org/10.1139/x03-240.

Marvin DC, Asner GP. Spatially explicit analysis of field inventories for national forest carbon monitoring. *Carbon Bal Manage* 2016;**11**:9. https://doi.org/10.1186/s13021-016-0050-0.

McDade LA, Bawa KS, Hespenheide HA. *et al.*, (eds.). *La Selva: Ecology and Natural History of a Neotropical Rain Forest*. Chicago, Illinois: University of Chicago Press, 1994, 493.

McTague, JP. New and composite point sampling estimates. *Can J For Res* 2010:**40**:2234–42. https://doi.org/10.1139/X10-158.

McRoberts RE, Tomppo EO. Remote sensing support for national forest inventories. *Remote Sens Environ* 2007;**110**:412–9. https://doi.org/10.1016/j.rse.2006.09.034.

Mesavage C, Grosenbaugh LR. Efficiency of several cruising designs on small tracts in North Arkansas. *J For* 1956;**9**:569–76. https://doi.org/10.1093/jof/54.9.569.

Mora-Espinoza JA, Peñalver-Romeo A, Aguilar-Torres FJ. *et al.* Angle sampling method for the inventory of teak plantations (Tectona grandis L. f). *Revista Chapingo* 2020;**26**:419–32. https://doi.org/10.5154/r.rchscfa.2019.11.081.

Nam VT, Anten NPR, van Kuijk M. Biomass dynamics in a logged forest: The role of wood density. *J Plant Res* 2018;**131**:611–21. https://doi.org/10.1007/s10265-018-1042-9.

Netto SP, Pelissari AL, Cysneiros VC. *et al.* Sampling procedures for inventory of commercial volume tree species in Amazon Forest. *An Acad Bras Cienc* 2017;**89**:1829–40. https://doi.org/10.1590/0001-3765201720160760.

Netto SP, Tello JCR, Wandresen RR. Size and shape of sample units in native forests and plantations. *Open J For* 2014;**4**:379–89. https://doi.org/10.4236/ojf.2014.44043.

Oliveira GMV, de Mello JM, de Lima RR. *et al.* Size and shape of experimental plots for Eremanthus erythropappus. *Cerne* 2011;**17**: 327–38. https://doi.org/10.1590/S0104-77602011000300006.

Packard KC, Radke PJ. Forest sampling combining fixed and variable radius sample plots. *Can J For Res* 2007;**37**:1460–71.

Palace MW, Sullivan FB, Ducey MJ. *et al.* Estimating forest structure in a tropical forest using field measurements, a synthetic model and discrete return lidar data. *Remote Sens Environ* 2015;**161**:1–11. https://doi.org/10.1016/j.rse.2015.01.020.

Palace M, Sullivan FB, Ducey MJ. *et al.* Estimating tropical forest structure using a terrestrial lidar. *PloS One* 2016;**11**:e0154115. https://doi.org/10.1371/journal.pone.0154115.

Pan C, Shrestha A, Innes JL. *et al.* Key challenges and approaches to addressing barriers in forest carbon offset projects. *J For Res* 2022;**33**:1109–22. https://doi.org/10.1007/s11676-022-01488-z.

Pasgaard M, Sun Z, Muller D. *et al.* Challenges and opportunities for REDD+: A reality check from perspectives of effectiveness, efficiency and equity. *Environ Sci Policy* 2016;**63**:161–9. https://doi.org/10.1016/j.envsci.2016.05.021.

Picard N, Gamarra JGP, Birigazzi L. *et al.* Plot-level variability in biomass for tropical forest inventory designs. *For Ecol Manage* 2018;**430**:10–20. https://doi.org/10.1016/J.FORECO.2018.07.052.

Pinto LOR, de Souza CR, Terra MCNS. *et al.* Optimal plot size for carbon-diversity sampling in tropical vegetation. *For Ecol Manage* 2021;**482**:118778. https://doi.org/10.1016/j.foreco.2020.118778.

Piponiot C, Anderson-Teixeira KJ, Davies SJ. *et al.* Distribution of biomass dynamics in relation to tree size in forests across the world. *New Phytol* 2022;**234**:1664–77. https://doi.org/10.1111/nph.17995.

Piponiot C, Condit R, Hubbell SP. *et al.* In: Muller-Landau HC, Wright SJ, (eds.). *Woody Biomass Stocks and Fluxes in the Barro Colorado Island 50-ha Plot. Chapter 53 in the First 100 Years of Research on Barro Colorado: Plant and Ecosystem Science*. Washington, D.C.: Smithsonian Institution Scholarly Press, 2024, 475–85. https://doi.org/10.5479/si.26882404.

Polley H, Schmitz F, Hennig P, Kroiher F. Individual country reports: Germany. In: *National Forest Inventories - pathways for common reporting*. E. Tomppo, T. Gschwantner, M. Lawrence and R.E. McRoberts (eds) 2010. New York: Springer, 612 pp. https://doi.org/10.1007/978-90-481-3233-1.

Pulkkinen M. On non-circularity of tree stem cross-sections: Effect of diameter selection on cross-section area estimation, Bitterlich sampling and stem volume estimation in scots pine. *Silva Fennica* 2012;**46**:924. https://doi.org/10.14214/sf.924.

R Core Team. *R: A Language and Environment for Statistical Computing*. Vienna, Austria: R Foundation for Statistical Computing, 2021 Available here: https://www.R-project.org/.

Roesch FA Jr. Adaptive cluster sampling for forest inventories. *For. Sci.* 1993;**39**:655–69.

Roveda M, Figueiredo Filho A, Pelissari AL. *et al.* Spatial continuity in a mixed ombrophilous forest with different size and shape of sample units. *Cerne* 2016;**22**:189–96. https://doi.org/10.1590/01047760201622022139.

Schreuder HT, Banyard SG, Brink GD. Comparison of three sampling methods in estimating stand parameters for a tropical forest. *For Ecol Manage* 1987;**21**:119–27. https://doi.org/10.1016/0378-1127(87)90076-4.

Schreuder HT, Gregoire TG, Wood GB. *Sampling Methods for Multiresource Forest Inventory*. New York: John Wiley & Sons, 1993, 446.

Slik JWF, Paoli G, McGuire K. *et al.* Large trees drive forest aboveground biomass variation in moist lowland forests across the tropics. *Glob Eco Biogeo* 2013;**22**:1261–71. https://doi.org/10.1111/geb.12092.

Smelko S. New view of the properties and applicability of the circular relascopic sample plots for the inventory and monitoring of the forest ecosystems. *Central Eur For J* 2013;**59**:1–18. https://doi.org/10.2478/v10114-011-0018-7.

Stephenson NL, Das AJ, Condit R. *et al.* Rate of tree carbon accumulation increases continuously with tree size. *Nature* 2014;**507**:90–3. https://doi.org/10.1038/nature12914.

Sullivan FB, Palace MW, Ducey MJ. Multivariate statistical analysis of asynchronous lidar data and vegetation models in a neotropical forest. *Remote Sens Environ* 2014;**154**:368–77. https://doi.org/10.1016/j.rse.2014.04.027.

Sullivan MJP, Talbot J, Lewis SL. *et al.* Diversity and carbon storage across the tropical forest biome. *Sci Rep* 2017;**7**:39102. https://doi.org/10.1038/srep39102.

Sullivan MJP, Lewis SL, Hubau W. *et al.* Field methods for sampling tree height for tropical forest biomass estimation. *Methods Ecol Evol* 2018;**9**:1179–89. https://doi.org/10.1111/2041-210X.12962.

Tomppo E, Henttonen H, Tuomainen T. Valtakunnan metsien 8. Inventoinnin menetelmä jatulokset metsäkeskuksittain Pohjois-Suomessa 1992–94 sekä tulokset Etelä-Suomessa 1986–92 ja koko maassa 1986–94. *Metsätieteen aikakauskirja* 2001;**1B**:99–248 https://doi.org/10.14214/ma.6434.

Tomppo E, Gschwantner T, Lawrence M. *et al.*, (eds.). *National Forest Inventories – Pathways for Common Reporting*. New York: Springer, 2010, 612 pp. https://doi.org/10.1007/978-90-481-3233-1.

Tomppo E, Heikkinen J, Henttonen HM. *et al.* 2011 Designing and conducting a forest inventory – Case: 9th national forest inventory of Finland. *Manag For Ecosys* **22.** Springer, Dordrecht, 270 https://doi.org/10.1007/978-94-007-1652-0.

Tomppo E, Malimbwi R, Katila M. *et al.* A sampling design for a large area forest inventory: Case Tanzania. *Can J For Res* 2014;**44**:931–48. https://doi.org/10.1139/cjfr-2013-0490.

Torres AB, Lovett JC. Using basal area to estimate aboveground carbon stocks in forests: La primavera Biosphere's reserve, Mexico. *Forestry* 2013;**86**:267–81. https://doi.org/10.1093/forestry/cps084.

Van Deusen PC, Grender JM. An alternative estimator for horizontal point clusters. *For Sci* 1989;**35**:257–62. https://doi.org/10.1093/forestscience/35.1.257.

Walker SM, Pearson TRH, Casarim FM. *et al. Standard Operating Procedures for Terrestrial Carbon Measurement, Version 2018*. Arlington, Virginia: Winrock International, 2018, 95.

Wensel LC, Levitan J, Barber K. Selection of basal area factor in point sampling. *J For* 1980;**78**:83–4. https://doi.org/10.1093/jof/78.2.83.

Wiant Jr HV, Yandle DO, Andreas R. Is BAF 10 a good choice for point sampling? *N J Appl For* 1984;**2**:23–5. https://doi.org/10.1093/njaf/1.2.23.

Winrock International. 2025 Available here: https://winrock.org/projects/leaf/

Yim JS, Shin MY, Son Y. *et al.* Cluster plot optimization for a large area forest resource inventory in Korea. *For Sci Technol* 2015;**11**:139–46. https://doi.org/10.1080/21580103.2014.968222.

Zanne AE, Lopez-Gonzalez G, Coomes DA. *et al.* Data from: Towards a worldwide Wood economics Spectrum [dataset]. *Dryad* 2009;**12**:351–66. https://doi.org/10.5061/dryad.234.

Zeide B. Plot size optimization. *For. Sci.* 1980;**26**:251–7. https://doi.org/10.1093/forestscience/26.2.251.

Forestry: An International Journal of Forest Research, 2025, 1–16
https://doi.org/10.1093/forestry/cpaf034
Original Article